# A microfluidic multi-injector for gradient generation

**Bong Geun Chung,† Francis Lin† and Noo Li Jeon***

***Received 7th September 2005, Accepted 13th March 2006***
***First published as an Advance Article on the web 6th April 2006***
**DOI: 10.1039/b512667c**

This paper describes a microfluidic multi-injector (MMI) that can generate temporal and spatial concentration gradients of soluble molecules. Compared to conventional glass micropipette-based methods that generate a single gradient, the MMI exploits microfluidic integration and actuation of multiple pulsatile injectors to generate arbitrary overlapping gradients that have not previously been possible. The MMI device is fabricated in poly(dimethylsiloxane) (PDMS) using multi-layer soft lithography and consists of fluidic channels and control channels with pneumatically actuated on-chip barrier valves. Repetitive actuation of on-chip valves control pulsatile release of solution that establishes microscopic chemical gradients around the orifice. The volume of solution released per actuation cycle ranged from 30 picolitres to several hundred picolitres and increased linearly with the duration of valve opening. The shape of the measured gradient profile agreed closely with the simulated diffusion profile from a point source. Steady state gradient profiles could be attained within 10 minutes, or less with an optimized pulse sequence. Overlapping gradients from 2 injectors were generated and characterized to highlight the advantages of MMI over conventional micropipette assays. The MMI platform should be useful for a wide range of basic and applied studies on chemotaxis and axon guidance.

## I. Introduction

Important developmental and physiological processes, such as axon guidance and immune response, are influenced by gradients of soluble factors such as chemokines and growth factors.[1,2] For example, microscopic differences in chemoattractant concentrations[3–5] in tissues can direct immune and cancer cell migration, thus playing an important role in host defense[6,7] and cancer metastasis.[8] Glass micropipette-based assays have been widely used to investigate the mechanism behind fundamental processes such as axon guidance,[9,10] cancer cell chemotaxis,[11–14] and yeast polarization.[15,16] Although stable and well-defined gradients can be obtained, micropipette-based assays are technically demanding to perform and not compatible with high-throughput experimentation. A reproducible experimental platform that can generate stable, multiple arbitrary gradients is needed for a range of basic and applied investigations in cell biology.

Recently, microfluidic gradient generators that provide improvements in gradient stability[17–20] compared to conventional assays, such as Boyden chambers, have been developed. Our group has used these microfluidic devices in investigation of neutrophil[21–23] and metastatic cancer cell[24] chemotaxis, as well as neural stem cell differentiation.[25] Although useful for many cell-based applications, an important limitation of the microfluidics-based approach is that the gradient can only be maintained within a microchannel with constant flow. Due to this experimental setup, migrating cells are constantly exposed to shear stress,[26] and they cannot be accessed directly from outside using techniques such as patch clamping. In addition, because the gradients are limited in a direction perpendicular to the flow, overlapping gradients at different angles cannot be obtained (only superimposed gradients). This paper describes a method for generating dynamically controlled gradients using microfabricated injectors on a single device by combining the functionalities of glass micropipette-based assays with integrated microfluidic components.

*Department of Biomedical Engineering, University of California at Irvine, Irvine, CA, 92697, USA. E-mail: njeon@uci.edu; Fax: +1-949-824-9968; Tel: +1-949-824-9032*
† These two authors contributed equally.

## II. Materials and methods

### Fabrication of MMI

The MMI was fabricated in PDMS (Sylgard 184, Dow Corning, MI) using multi-layer soft lithography.[27] It consists of round, 10 μm thick fluidic channels and 40 μm thick control channels. The master mold for the fluidic channel was fabricated by patterning 10 μm thick positive photoresist (Shipley SJR-5740, MicroChem, MA) on a Si wafer (Silicon Inc., ID). After development, the resist was reflowed at 200 °C for 30 min to obtain a round profile.[27] The master mold for the pressurized control layer was fabricated by patterning 40 μm thick negative photoresist (SU-8 50, MicroChem, MA). A replica of the fluidic channel was obtained by spin-coating PDMS at 2000 rpm for 60 s followed by baking at 80 °C for 1.5 h. This resulted in a 25 μm thick PDMS membrane containing the fluidic channels. A thick replica of the control channels and the PDMS membrane containing fluidic channels were treated with oxygen plasma (model PDC-001, Harrick Scientific, NY) for 2 min and brought together to form an irreversible seal. The inlets and outlets of the channels were punched out using sharpened needle tips. A reservoir was cut out of the device by severing a microchannel to render a 10 μm orifice. The assembled PDMS piece with fluidic channel and

 

control channel was bonded with a glass slide (Corning, NY) to complete the device.

### Experimental setup

Actuation and control of the MMI device was performed using a previously reported setup.[27,28] Briefly, fluidic channels filled with PBS (wash channel) and FITC-Dextran (1 mM, MW = 10 kDa, Sigma) were connected to a 3 psi pressure source. The crossing of a control channel over the fluidic channel formed the on-chip barrier valve that was actuated by pressurizing the control channel with 10 psi pressure. When the valve was opened by venting the control channel, a small volume of FITC-Dextran solution was released into the reservoir through a 10 μm orifice. The reservoir (40 mm × 10 mm × 2.5 mm) contained 1 mL of buffer solution.

The MMI devices could be used to generate stable gradients for as long as 2–3 h. This time could be increased with a larger reservoir to minimize increasing baseline concentration (each pulse delivers ~70 pL of 1 mM dye solution or ~80 nL over 30 min, the net increase in base concentration in the reservoir with 1 mL is negligible). In our experience, larger reservoirs were more difficult to work with because convective flows generated by thermal gradients severely affected the gradient profiles. Greater than 90% of the fabricated devices were functional, and no variations were observed between different batches of devices. To minimize variables, all devices were used immediately after fabrication (while all sides of the channels were made hydrophilic after plasma treatment) and new MMI devices were fabricated for each experiment. Gradient profiles generated from the devices were repeatable and reproducible.

### Image acquisition and analysis

Fluorescence micrographs of gradients were taken using an inverted microscope (Nikon TE300) with a digital CCD camera (CoolSNAP cf, Roper Scientific, AZ). The microscope and CCD camera were controlled with MetaMorph (Universal Imaging, PA). Gradient profiles were analyzed using MetaMorph and MATLAB (The Mathworks, MA).

## III. Results and discussion

### MMI design

The MMI was designed to integrate the functionalities of pressure-actuated glass micropipettes on a single device using microfabrication and multi-layer soft lithography. To generate a microscopic gradient, we fabricated a device with a network of fluidic channels that was controlled with a set of pressure control channels. Steady ejection of a chemical solution from a microchannel-based orifice into a large reservoir resulted in gradients similar to those produced by micropipettes.[9,10] In MMI, macroscopic pressure tubing and valves were replaced with pressure control channels and on-chip barrier valves, while the glass micropipette was replaced with a fluidic channel with a 10 μm orifice. Because several on-chip barrier valves can be readily integrated onto the microfluidic platform, it offers several advantages in controlling the flow and ejection of solutions to generate gradients. For example, multiple injectors can be fabricated on a single device as easily as a single injector, and can generate overlapping gradients of complex gradient profiles as demonstrated later in this work.

Fig. 1 shows the schematic of a representative MMI device. The device consists of fluidic channels and pressure control channels in PDMS that are separated by a 25 μm thick membrane. The entire device was bonded to a glass slide with fluidic channels formed against the glass bottom. An orifice and reservoir were formed by severing a microchannel and cutting out the piece of PDMS. The barrier valves (V1, V2, and V3) were formed at the control channel and fluidic channel crossings.

The fluid reservoirs were filled with dye solutions and connected to an external pressure source (3 psi). The barrier valves were cycled to release small amounts of fluorescent solution into the reservoir. These valves were actuated by applying positive pressure (10 psi) to the control channel. This caused the membrane between the channels to deform and close the fluidic channel. Venting the pressure channel opened the underlying fluidic channel for fluid flow. Repetitive actuation of the barrier valve allowed ejection of picolitre amounts of fluorescent solution into the reservoir. Similar to a micropipette, steady pulsatile release of solution from an orifice resulted in stable gradients around the orifice.

### Measurement of release volume

In order to characterize the steady state gradient generated with the MMI, we measured the volume of the ejected solution per actuation cycle as a function of valve opening duration. The valve opening duration is directly proportional to the time when the air pressure is withdrawn from the control channel. The average volume was determined by measuring the diameter of oil droplets ejected into the water reservoir using a previously reported method.[9,10] We measured the diameter

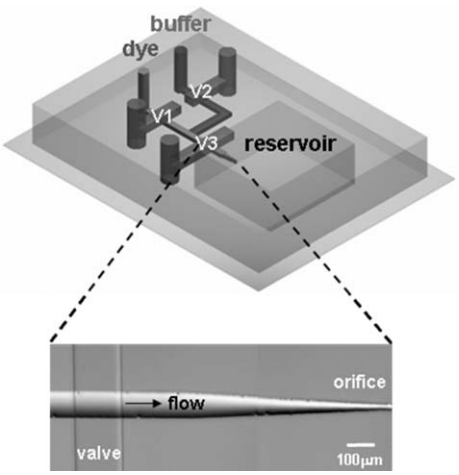


**Fig. 1** Schematic design of the Microfluidic Multi-Injector (MMI). Control channel and fluidic channel crossings make up the on-chip barrier valves (V1, V2, V3). These valves were actuated by pressurizing the control channel and deforming the membrane between the channels to close the fluidic channel. These valves controlled the pulsatile release of solution into the reservoir to generate a gradient. The micrograph shows the region around the barrier valve and the microfluidic orifice.

of the droplets ($n$ = 50 droplets per condition) and averaged the results from 5 different devices to calculate the volume. The smallest volume that could be measured per actuation cycle was ~30 pL, at a 0.5 s opening duration. For valve open durations shorter than 0.5 s, no measurable droplets were produced. The measured volume of oil droplets may have been affected by surface effects and may be slightly different for cases of miscible solutions (*i.e.* aqueous droplet ejection into an aqueous reservoir such as FTIC-Dextran solution into PBS).

The volume of solution ejected *via* a 10 μm semicircular orifice increased linearly as a function of valve opening time ($R$ = 0.996, Fig. 2). The size of the microfluidic orifice was significantly larger than glass micropipettes, resulting in a larger average volume (30 pL *vs.* 1 pL).[9,10] This result illustrated that active control of valve opening duration can be used to control the volume of solution ejected, and that microfabricated MMIs can be used to produce stable gradients.

### Generation of steady state concentration gradient

The release volume must be accurately controlled with the valves to minimize macroscopic fluid flow and fluctuations in gradient profile. Building on the results obtained in previous section, valve opening times and frequency were optimized to avoid rippling fluctuations in gradients. Fig. 3 shows the development of a stable gradient as a function of time for valve actuation at 0.67 Hz with 1 s opening. To quantitatively analyze the concentration gradient of the ejected substance, we used FITC-Dextran solution and measured the fluorescence intensity near the microfluidic orifice. Fig. 3A depicts the 2D fluorescence intensity profiles at various times after the start of pulsatile release. The profile was governed by diffusion from a point source and reached steady state after 10 min. Fig. 3B shows the normalized fluorescence intensity profile along a horizontal line near the orifice. The measured fluorescence intensity profiles after 10 and 30 min fit well with the diffusion profile predicted by simulation.

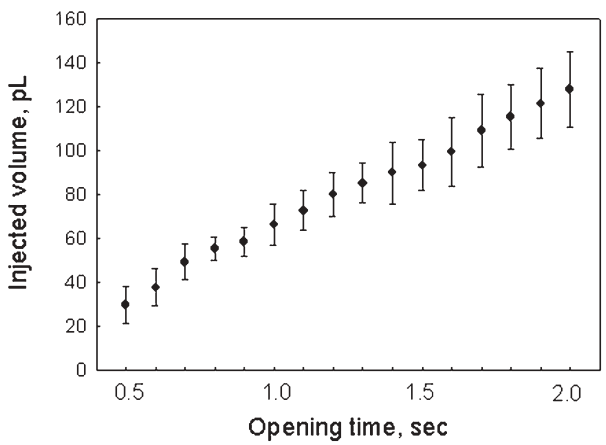


**Fig. 2** Graph showing the volume of the ejected solutions as a function of valve opening time. The volume of the ejected solution ranged from 30 pL to 130 pL and increased linearly with the length of opening duration.

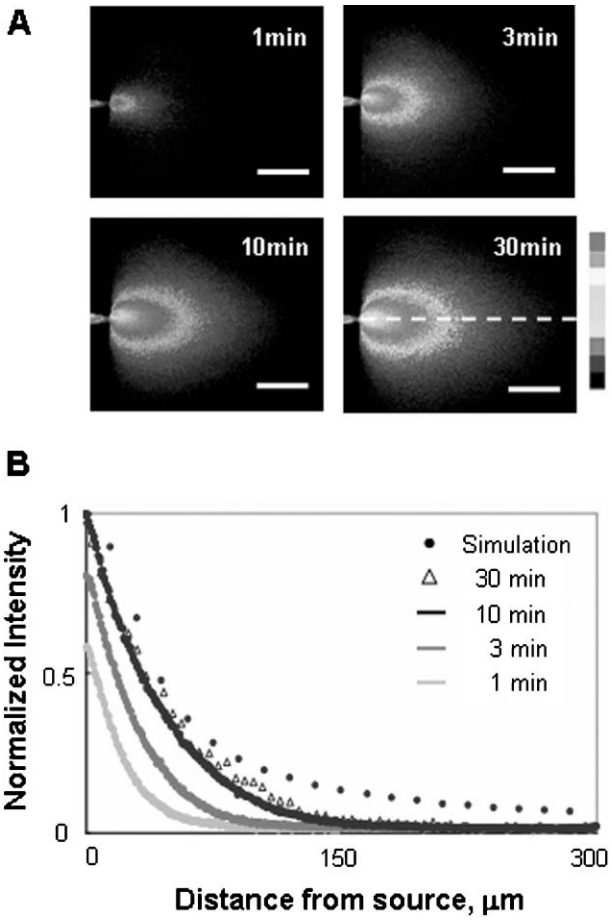


**Fig. 3** Steady state concentration gradients generated by pulsatile ejection of solution in the MMI. (A) 2D intensity profiles show the gradient generations of FITC-Dextran and its evolution with time. The barrier valve was actuated at 0.67 Hz and opened for 1 s. (B) 1D normalized fluorescence intensity profile along a horizontal line of Fig. 3A. The steady state gradients were achieved within 10 min. The experimental measurements closely agreed with simulations. Scale bars represent 50 μm.

The concentration gradients generated in the MMI were simulated using an approach that was used for the glass micropipette-based method.[9,10] The concentration gradient produced by repetitive ejection of the solution was calculated by summing the concentration profile from each pulse. The concentration profile after $n$ injections was expressed as:

$$C(r,t) = \sum_{i}^{n} \frac{q e^{\frac{-r^2}{4D(t-it_0)}}}{4[\pi D(t-it_0)]^{\frac{3}{2}}}$$

where $C(r,t)$ is the concentration at position $r$ relative to the injector and time $t$ after the onset of ejections, $i$ is an integer from 0 to $n$, $t_0$ is the inverse of ejection frequency, $q$ is a constant, and $D$ is the diffusion constant. For our experiments, $t_0$ was 1.5 s for a pulse of FITC-Dextran ejected every 0.5 s by opening the valves for 1 s. From Fig. 2, the volume of a single ejection is approximately 66.5 pL for $t_0$ = 1.5 s (valve opening duration = 1 s). The constant $q$ was eliminated after normalization; $D$ for FITC-Dextran was approximated at $1.7 \times 10^{-6}$ cm$^2$ s$^{-1}$ in diluted solution at room temperature.

The calculated concentration profiles at 10 min and 30 min agreed closely with experimental results, as shown in Fig. 3B. Experimentally measured fluorescence profiles were compared with simulated profiles at 10 min by an F-test using the Origin software package, and showed no statistically significant difference ($p$ = 0.32). The calculated and experimentally measured concentration gradients were normalized to the highest concentration before comparison.

Because the injector is located at the bottom of the reservoir, the gradient formed around the injector tip is radial. In our experiment, we have measured the fluorescence profile using an epifluorescence microscope. The measured value is a sum of the fluorescence over the entire depth of the reservoir ($h$ = 2.5 mm) and may differ slightly from the actual gradient that is present immediately above the substrate. Fortunately, since the gradient decays rapidly away from the tip reaching baseline at around 150 μm, the difference between the measured intensity and simulated value should be minimal, as the summed fluorescence is over ~150 μm height above the surface. In addition, the deviation will be more pronounced closer to the tip of the injector and will progressively become less important around the periphery. For applications with mammalian cells, the region where there is steep change in the slope is of most interest, which is about ~100 μm away from the tip. Hence the effect of the difference between measured intensity and the simulated value will be minimal.

A steady state gradient was formed within 10 min over a few hundred micrometres from the point source. Controlled pulsatile release minimized flow of solution and gradient fluctuations. The opening duration and actuation frequency of the barrier valve can have a significant influence on concentration gradient profiles. Pulsatile release of a small volume of solution, produced by a short opening duration (1 s) and a delay (0.5 s), resulted in stable gradients. The gradient could be maintained as long as continuous pulsatile ejection was applied. The time to establish steady state gradients can be shortened using different pulsing sequences. When a longer valve opening duration is followed by progressively shorter opening durations, steady state gradients can be obtained in less than 3 min (data not shown).

In order to generate a stable concentration gradient by pulsatile injection, each pulse of injected solution must readily diffuse out into the buffer reservoir. This condition also requires that the total amount of chemical substance injected into the reservoir be significantly less than the total buffer volume, to avoid an increase in baseline concentration. Under our experimental conditions, about ~70 pL of 1 mM FITC-Dextran solution is injected at 0.67 Hz. Therefore, over 30 min, a total of 80 nL of FITC-Dextran is added into the reservoir. This amount is significantly smaller than the total volume of the reservoir (1 mL). Under this constraint, each injection can be modeled as an independent point-source diffusion process in an infinite reservoir, and the spatial distribution of the released FITC-Dextran at a given time-point can be obtained by summing up the concentration profiles of each ejection, as discussed earlier. The steady state concentration gradient results from the equilibrium of the spatio-temporal evolution of all the profiles. At the same time, to obtain optimal valve opening and delay combination, ejection rate (influenced by opening time) needs to be balanced with decay time (influenced by delay time).

Preliminary experiments indicated that after a single injection (1 s opening), it takes ~5 s for the fluorescence to completely decay by diffusion. In addition, as shown in Fig. 2, the opening time needs to be longer than 0.5 s to observe a measurable injection volume. These values were used as starting points to optimize the open/delay times. In extreme cases, when the opening was significantly longer than the delay time, it took a long delay to reach equilibrium. This was caused by a large injected volume, from the long opening, that increased the baseline concentration with each additional opening. At the other extreme, a short opening followed by a long delay caused large fluctuations in concentration, as each pulse had decayed considerably before the next injection.

### Generation of overlapping gradients using MMI

To demonstrate the potential of integrating multiple injectors to produce complex superimposed gradients, we have fabricated a dual injector on a single chip. This device is capable of producing two identical gradients, or two different competing gradients, simultaneously. This device is an illustration of how multiple injectors can be combined to produce complex gradients. By fabricating a number of injectors in parallel, as well as in arbitrary positions, we should be able to generate complex gradients. Fig. 4A shows the schematic design of the

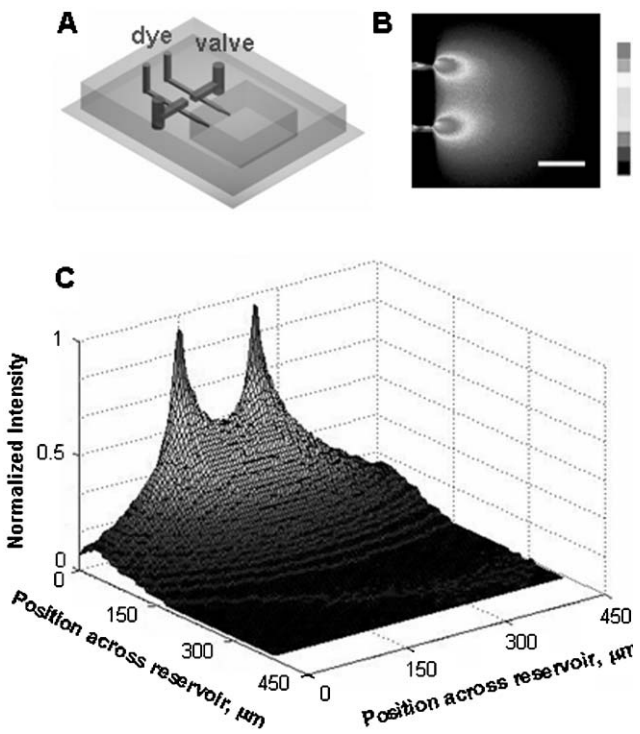


**Fig. 4** Generation of overlapping gradients in the MMI. (A) Schematic design of the parallel MMI on a single chip. Two parallel micro-injectors, 120 μm apart, were simultaneously controlled by valves actuated at 0.67 Hz with 1 s opening. (B) 2D intensity profile of the fluorescence image showing symmetric overlapping gradients of FITC-Dextran. (C) 3D normalized fluorescence intensity profile. Scale bar represents 100 μm.

MMI device that can produce overlapping gradients. Different overlapping gradient profiles can be generated by fabricating multiple injectors on a single chip for high-throughput experiments. Fig. 4B shows the 2D fluorescence intensity profile of overlapping gradients. Symmetric, overlapping gradients were formed simultaneously. The fluorescence intensity of the overlapping gradients was visualized by 3D contour plots, as shown in Fig. 4C.

The MMI has several advantages over conventional micropipette assays and microfluidic mixer devices for generating complex overlapping gradients. Compared to conventional micropipette-based gradients, generating superimposed and overlapping gradients of arbitrary configurations is relatively straightforward with the MMI. Because several injectors can be designed and fabricated with integrated control valves, reproducible results are obtained independent of the number of valves. Because they are fabricated by replica molding, multiple devices can be prepared in parallel. This allows for single use devices with multiple backup chips. In addition, compared to the serpentine channel microfluidic mixers, overlapping gradients at different angles can be rapidly established and dynamically controlled without a complex network of channels.

The opening duration, actuation frequency of the on-chip barrier valve and backpressure can play an important role in symmetric and asymmetric overlapping gradients. If the opening duration of the valves is individually controlled using different frequencies, asymmetric overlapping gradients can be formed. Similarly, application of different backpressures to dual injectors will also result in non-symmetric gradients. Because each injector can be controlled independently, it is possible to generate dynamic spatio-temporal gradients. For example, gradient direction and shape can be switched easily by controlling the appropriate injectors in an array. When opposing micro-injectors are alternately turned on and off, cells can be stimulated by competing gradients of chemoattractants and chemorepellents.

## IV. Conclusion

This paper reports a microfluidic multi-injector device that combines functionalities of glass micropipette-based assays with integrated microfluidic valves on a single chip. Pulsatile release of solution using integrated valves in PDMS produced microscopic chemical gradients near the orifice. The amount of solution released per actuation cycle was measured and optimized to generate a stable gradient. One of the main advantages of this device is that dynamic temporal and spatial gradients are achieved reliably using a simple experimental setup. Miniaturized integration of multiple injectors on a single device will allow reproducible, high-throughput experiments with spatio-temporal gradients, with potential applications in basic and applied studies in chemotaxis and axon guidance.


## Acknowledgements

We thank S. Sanga for assistance with MATLAB. We also thank the referees for helpful comments.


## References


1 D. Bray and P. J. Hollenbeck, *Annu. Rev. Cell Biol.*, 1988, **4**, 43–61.
2 M. Baggiolini, B. Dewald and B. Moser, *Annu. Rev. Immunol.*, 1997, **15**, 675–705.
3 C. Janetopoulos, L. Ma, P. N. Devreotes and P. A. Iglesias, *Proc. Natl. Acad. Sci. U. S. A.*, 2004, **101**, 8951–8956.
4 E. F. Foxman, J. J. Campbell and E. C. Butcher, *J. Cell Biol.*, 1997, **139**, 1349–1360.
5 E. F. Foxman, E. J. Kunkel and E. C. Butcher, *J. Cell Biol.*, 1999, **147**, 577–588.
6 S. Zigmond, *J. Cell Biol.*, 1977, **75**, 606.
7 P. Kubes, *Sem. Immunol.*, 2002, **14**, 65–72.
8 L. V. Dekker and A. W. Segal, *Science*, 2000, **287**, 982–985.
9 J. Zheng, M. Felder, J. Connor and M. Poo, *Nature*, 1994, **368**, 140–144.
10 A. Lohof, M. Quillan, Y. Dan and M. Poo, *J. Neurosci.*, 1992, **12**, 1253–1261.
11 J. Condeelis, R. Singer and J. E. Segall, *Annu. Rev. Cell Dev. Biol.*, 2005, **21**, 695–718.
12 H. Yamaguchi, J. Wyckoff and J. Condeelis, *Curr. Opin. Cell Biol.*, 2005, **17**, 1–6.
13 C. Y. Chung, S. Funamoto and R. A. Firtel, *Trends Biochem. Sci.*, 2001, **26**, 557–566.
14 L. Soon, G. Mouneimne, J. Segall, J. Wyckoff and J. Condeelis, *Cell Motil. Cytoskeleton*, 2005, **62**, 1, 27–34.
15 J. E. Segall, M. Manson and H. Berg, *Nature*, 1982, **296**, 855–857.
16 J. E. Segall, *Proc. Natl. Acad. Sci. U. S. A.*, 1993, **90**, 8332–8336.
17 G. M. Whitesides, E. Ostuni, S. Takayama, X. Jiang and D. E. Ingber, *Annu. Rev. Biomed. Eng.*, 2001, **3**, 335–373.
18 N. L. Jeon, S. K. W. Dertinger, D. T. Chiu, I. S. Choi, A. D. Stroock and G. M. Whitesides, *Langmuir*, 2000, **16**, 8311–8316.
19 S. K. W. Dertinger, D. T. Chiu, N. L. Jeon and G. M. Whitesides, *Anal. Chem.*, 2001, **73**, 1240–1246.
20 F. Lin, W. Saadi, S. W. Rhee, S. Wang, S. Mittal and N. L. Jeon, *Lab Chip*, 2004, **4**, 164–167.
21 N. L. Jeon, H. Baskaran, S. K. W. Dertinger, G. M. Whitesides, L. V. D. Water and M. Toner, *Nat. Biotechnol.*, 2002, **20**, 826–830.
22 F. Lin, C. M. Nguyen, S. Wang, W. Saadi, S. P. Gross and N. L. Jeon, *Biochem. Biophys. Res. Commun.*, 2004, **319**, 576–581.
23 F. Lin, C. M. Nguyen, S. Wang, W. Saadi, S. P. Gross and N. L. Jeon, *Ann. Biomed. Eng.*, 2005, **33**, 4, 475–482.
24 S. Wang, W. Saadi, F. Lin, C. M. Nguyen and N. L. Jeon, *Exp. Cell Res.*, 2004, **300**, 180–189.
25 B. G. Chung, L. A. Flanagan, S. W. Rhee, P. H. Schwartz, A. P. Lee, E. S. Monuki and N. L. Jeon, *Lab Chip*, 2005, **5**, 401–406.
26 G. M. Walker, J. Sai, A. Richmond, M. Stremler, C. Y. Chung and J. P. Wikswo, *Lab Chip*, 2005, **5**, 6, 611–618.
27 M. A. Unger, H. P. Chou, T. Thorsen, A. Scherer and S. R. Quake, *Science*, 2000, **288**, 113–116.
28 T. Thorsen, S. J. Maerkl and S. R. Quake, *Science*, 2002, **298**, 580–584.